

# We are IntechOpen, the world's leading publisher of Open Access books Built by scientists, for scientists

4,800

Open access books available

122,000

International authors and editors

135M

Downloads

Our authors are among the

154

Countries delivered to

TOP 1%

most cited scientists

12.2%

Contributors from top 500 universities



WEB OF SCIENCE™

Selection of our books indexed in the Book Citation Index  
in Web of Science™ Core Collection (BKCI)

Interested in publishing with us?  
Contact [book.department@intechopen.com](mailto:book.department@intechopen.com)

Numbers displayed above are based on latest data collected.  
For more information visit [www.intechopen.com](http://www.intechopen.com)



# Origin and Detection of Actinides: Where Do We Stand with the Accelerator Mass Spectrometry Technique?

Mario De Cesare

*CIRCE - INNOVA, Dipartimento di Scienze Ambientali - II Università di Napoli, Caserta  
Italia*

## 1. Introduction

The activation products in a reactor's primary coolant loop is a main reason why Nuclear Power Plants (NPPs) use a chain of two or three coolant loops linked by heat exchangers, but isolated against matter exchange. However, during routine operations, damages are likely to occur, and the formation of micro-cracks represents a way of leakage for activation products. Through the same way, also leakage of material directly from the reactor core can take place: fission products and several isotopes of actinides,  $^{235}\text{U}$ ,  $^{238}\text{U}$ ,  $^{239}\text{Pu}$  and those heavier isotopes produced by single and multiple neutron capture on them. The explosion of a nuclear bomb leads itself to releases of radioactive material, which, in this case, could be widespread in the environment up to a global scale.

Moreover, undeclared nuclear activities and/or illegal use and transport of nuclear fuel can be detected through determination of the isotopic ratios of U and Pu in such samples. As all the activities related to nuclear technology have been, since the second half of the past century, responsible of changes in the concentration of the anthropogenic radionuclides over global scale, it would be not inappropriate referring to a further Global Environmental Change which is recognizable within every environmental matrix: soil, superficial and ground-waters and living organisms. The outcome of the interactions of ionizing particles with living matter is, already, unluckily, well known, that's why a number of studies have been flourishing in order to assess the radiological risk, by analyzing the environmental pathways of radionuclides and their behavior within the human food chain. In parallel, accurate assessment and monitoring of every source of radioactive contamination are required from the point of view of the prevention from this new scenario of radiological exposition (Quinto, 2007). Quantifying the releases and tracing their dispersion in the environment has traditionally been the task of Alpha Spectrometry (AS (O'Donnell et al., 1997; Sanchez et al., 1992) or, more recently, of Inductively Coupled Plasma Mass Spectrometry (ICP-MS) (Ketterer et al., 2003; Ketterer & Szechenyi, 2008; Wyse et al., 2001) or Thermal Ionization (TI-MS) (Beasley et al., 1998; Richter et al., 1999). Although these are mature methodologies, each has its limitations, which are largely surmounted by the relatively new technique of Accelerator Mass Spectrometry (AMS) (Fifield, 2008; Steier et al., 2010). In the chapter the origin of actinides is discussed as well as the potential of actinides to serve as a tracer for geomorphologic processes and as sensitive

fingerprints of releases from nuclear facilities (Quinto et al., 2009; Sakaguchi et al., 2009; Steier et al., 2008).

Moreover the sensitivity of the different actinides measurements method and the peculiarity of the AMS technique with respect to AS and CMS techniques are illustrated. Furthermore the principles and methodology of heavy-element AMS as applied to U and Pu isotopes are described, and the ways in which these have been implemented in various laboratories around the world are discussed with particular attention to the CIRCE (Center for Isotopic Research on Cultural and Environmental Heritage) and ANU (Australian National University) accelerator facilities (Fifield et al., 1996; Terrasi et al., 2007).

## 2. Origin and detection of actinides

### 2.1 Sources of contamination

The discovery of the fission properties of  $^{235}\text{U}$  and  $^{239}\text{Pu}$  and the capability to sustain chain fission reactions, have opened the way to several applications of nuclear energy. Nuclear Power Plants are used to generate thermal, and then electric, power, while Nuclear Weapons use the destructive effects of supercritical chain reactions. Both of these applications of nuclear energy, together with all the activities correlated with production, transport and reprocessing of nuclear fuel, lead to releases of a wide range of radioactive elements in the environment.

The free neutrons produced by fission are partly adsorbed by other nuclei of fissile material, allowing, in the appropriate conditions, the self-sustainability of the chain reaction, and partly adsorbed by other elements in the air and the ground, during fission in nuclear explosions, and by structural and cladding materials and coolant circuits, during the exercise phase of NPP. The production of activation products in a reactor's primary coolant loop is a main reason why NPPs use a chain of two or three coolant loops linked by heat exchangers, but isolated against matter exchange. However, during routine operations, damages are likely to occur, and the formation of micro-cracks represents a way of leakage for activation products. Through the same way, also leakage of material directly from the reactor core can take place: fission products and several isotopes of actinides,  $^{235}\text{U}$ ,  $^{238}\text{U}$ ,  $^{239}\text{Pu}$  and those heavier isotopes produced by single and multiple neutron capture on them. The input of these radionuclides in the outer coolant circuit results in their release in the environment within airborne and liquid effluents during the routine running of a NPPs. Of course, other ways of leakage would be accidents leading to uncontrolled explosions of the reactor or any kind of exceptional damage at various structural devices. The diffusion area of contamination from routine exercise of NPPs is restricted to a local scale, affecting the surroundings, the river or artificial channel, which provides and drains the reactor cooling water and the following areas connected with the river water circulation (Quinto, 2007). On the some grounds, the above radionuclides can be dispersed in the environment by the explosions of nuclear weapons in the atmosphere or underground.

Schematically it is possible to divide the sources of contamination into **large and small scale contamination**:

1. large scale source of radionuclide contamination includes the explosion of a Nuclear bomb. The contamination could be widespread in the environment up to a global scale. Several atmospheric nuclear tests conducted between 1945 and 1963 by the US and Soviet Union, by UK between 1952 and 1963, by France until 1974 and by the People's Republic of China until 1980, projected their debris into the stratosphere, from where, due to the global wind circulation, they have been deposited around the world within what is called **global fall**

| Actinides         | $T_{1/2}(y)$        | Emitted radiation |
|-------------------|---------------------|-------------------|
| $^{234}\text{U}$  | $2.5 \cdot 10^5$    | $\alpha$          |
| $^{235}\text{U}$  | $7.0 \cdot 10^8$    | $\alpha$          |
| $^{236}\text{U}$  | $23.0 \cdot 10^6$   | $\alpha$          |
| $^{238}\text{U}$  | $4.5 \cdot 10^9$    | $\alpha$          |
| $^{238}\text{Pu}$ | 88.0                | $\alpha$          |
| $^{239}\text{Pu}$ | $2.4 \cdot 10^4$    | $\alpha$          |
| $^{240}\text{Pu}$ | $6.6 \cdot 10^3$    | $\alpha$          |
| $^{241}\text{Pu}$ | 14                  | $\beta^-$         |
| $^{242}\text{Pu}$ | $3.8 \cdot 10^5$    | $\alpha$          |
| $^{243}\text{Pu}$ | $5.7 \cdot 10^{-4}$ | $\beta^-$         |
| $^{244}\text{Pu}$ | $82.0 \cdot 10^6$   | $\alpha$          |

Table 1. Half-lives,  $T_{1/2}$  and decay mode of Uranium and Plutonium isotopes in year, y, units.

- out.** Another large scale source of contamination is due to one of the worst accidents in the history of nuclear energy that occurred on 26 April, 1986, at the Chernobyl Nuclear Power Station near Kiev in Ukraine, affecting mainly Central and Northern Europe, although  $^{137}\text{Cs}$  was detectable even in Southern Italy (Roca et al., 1989).
2. small scale includes the operation and decommissioning activities of a NPP which could lead to airborne and liquid releases of radionuclides. At the same level, several steps in the fuel cycle, up to the reprocessing of spent fuel, can release activation and fission products, as well as the fissile material itself.

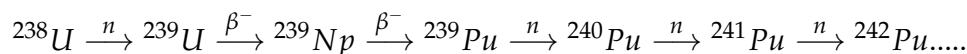
Obviously, given that the relative concentrations of plutonium and uranium isotopes depend on the nature of the source material and on its subsequent irradiation history, all these sources of contamination do not give the same contributions of contamination. As it will be shown in the following, useful tools to solve among different contributions are the isotopic ratios:  $^{236}\text{U}/^{238}\text{U}$ ,  $^{240}\text{Pu}/^{239}\text{Pu}$ ,  $^{242}\text{Pu}/^{239}\text{Pu}$ ,  $^{244}\text{Pu}/^{239}\text{Pu}$  and  $^{238}\text{Pu}/^{239+240}\text{Pu}$ .. Table 1 shows the half lives of the relevant isotopes of U and Pu.

2.2 Different contamination sources

The relative concentrations of plutonium and uranium isotopes depend on the nature of the source material and on its subsequent irradiation history; all these sources of contamination do not give the same contributions of contamination.

Here are shown some example of different contamination sources:

- Being fissile material,  $^{239}\text{Pu}$  is the most abundant isotope in weapon-grade plutonium. The average ratio of  $^{240}\text{Pu}/^{239}\text{Pu}$ , before detonation is  $^{240}\text{Pu}/^{239}\text{Pu} \leq 0.07$  while after detonation is  $^{240}\text{Pu}/^{239}\text{Pu} \simeq 0.35$  (Diamond et al., 1960), for the US tests. After detonation  $^{239}\text{Pu}$  isotope is still the most abundant because the ratio is always less than one.  $^{239}\text{Pu}$  is produced from  $^{238}\text{U}$  via neutron capture where  $^{238}\text{U}$  is the most abundant isotope of uranium in nature,  $^{238}\text{U} \simeq 99.275\%$ ,  $^{235}\text{U} \simeq 0.720\%$  and  $^{234}\text{U} \simeq 0.005\%$ . During detonation of nuclear weapons and running of nuclear reactors,  $^{239}\text{Pu}$  undergoes neutron capture to generate  $^{240}\text{Pu}$ , and also the heavier  $^{241}\text{Pu}$ ,  $^{242}\text{Pu}$  and  $^{244}\text{Pu}$  are produced through successive neutron captures. The resulting short-lived  $^{239}\text{U}$  ( $T_{1/2} = 23.45$  min) decays by  $\beta^-$  into  $^{239}\text{Np}$ , which in turn decays by  $\beta^-$  ( $T_{1/2} = 2.356$  days) into  $^{239}\text{Pu}$ :

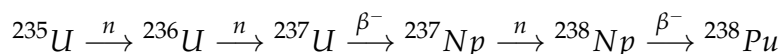


In weapon test fallout, the ratio  $^{240}\text{Pu}/^{239}\text{Pu}$  varies depending on the test parameters in the range of 0.10-0.35. The average for the Northern hemisphere is about 0.18, (Koide et al., 1985).

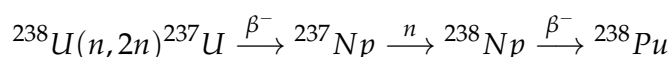
Significantly different values, in the range 0.035-0.05, are found in Mururoa and Fangataufa atoll sediment, because of the particular nature of French testing, (Chiappini et al., 1999) and (Hrneceka et al., 2005).

- In nuclear reactors, as mentioned before, due to the different composition of fuels, uranium enrichment and burn-up degree, characteristic relative abundances of plutonium isotopes will be obtained:  $^{240}\text{Pu}/^{239}\text{Pu}$  increases with irradiation time, which, in turn affects  $^{238}\text{Pu}/^{239+240}\text{Pu}$ .

$^{238}\text{Pu}$  is produced by neutron capture from  $^{237}\text{Np}$ , which is itself produced by two successive neutron captures from  $^{235}\text{U}$ :



or via the fast-neutron induced  $^{238}\text{U}(n,2n)^{237}\text{U}$  reaction:



The ratio  $^{238}\text{Pu}/^{239+240}\text{Pu}$  is useful to resolve between different sources in case they show similar  $^{240}\text{Pu}/^{239}\text{Pu}$ , e.g., irradiated nuclear fuel in a PWR (Pressurized Water Reactor) with 7-20% of  $^{235}\text{U}$  and burn-up 1.4-3.9 GW·d (GWatt·day) reaches  $^{240}\text{Pu}/^{239}\text{Pu}$  isotopic ratios of 0.13, a value, that could be ascribed also to global fall out. On the other side, these two sources show quite different  $^{238}\text{Pu}/^{239+240}\text{Pu}$  activity ratio, 0.025-0.04 for the global fallout and 0.45 for that nuclear fuel, (Quinto, 2007).

- Another valuable tool to identify a nuclear reactor origin of a radionuclide contamination is  $^{236}\text{U}/^{238}\text{U}$  isotopic ratio. The dominant  $^{236}\text{U}$  mode of formation is the capture of a thermal neutron by  $^{235}\text{U}$ , a secondary contribution being the alpha decay of  $^{240}\text{Pu}$ . Its concentration in nature has been heavily increased as a consequence of irradiation of enriched uranium in nuclear reactors. Several orders of magnitude of difference between the  $^{236}\text{U}/^{238}\text{U}$  isotopic ratios in naturally-occurring uranium ( $10^{-9}$  to  $10^{-13}$ ) and in spent nuclear fuel ( $10^{-2}$  to  $10^{-4}$ ) imply that also a small contamination from irradiated nuclear fuel in natural samples is able to increase significantly the  $^{236}\text{U}/^{238}\text{U}$  ratio measured in the whole sample.

### 2.3 Needs for actinides monitoring

The nuclear safeguard system used to monitor compliance with the Nuclear Non-proliferation Treaty relies to a significant degree on the analysis of environmental samples. Undeclared nuclear activities and/or illegal use and transport of nuclear fuel can be detected through determination of the isotopic ratios of U and Pu in such samples. Accurate assessment and monitoring of every source of radioactive contamination are required from the point of view of the prevention from radiological exposure.

Both the operations of decommissioning of the existing NPPs and the possible future operation of new plants demand accurate investigations about the possible contamination by radioactive releases of nuclear sites and neighboring territory and of structural



materials of the reactors. The monitoring activity of surveillance institutions uses assessed radiometric techniques, but more and more ultrasensitive methodologies for the detection and quantification of ultralow activity radionuclides is requested at international level.

Most of U and Pu isotopes are long lived alpha emitters with very low specific activity: their detection and the measurement of their concentration and isotopic abundance demands very high sensitivity, so that they are included among the so called "hardly detectable" radionuclides. As it will be shown in the following, the required sensitivity is often not achieved using conventional analytical techniques, such as counting of the radiation emitted in the decay or conventional mass spectrometry. The main task of the present work is to illustrate an ultrasensitive methodology for the detection of ultralow level radionuclides belonging to the actinides subgroup of the periodic table.

The method is based on a combination of AS and AMS: the reason for such a combination lies in the fact that it may be necessary to be able to measure the Pu isotopes at the fg level and the U isotopes where the total uranium content may be at the ng level or with a sensitivity as low as  $10^{-13}$  in the measurement of the  $^{236}\text{U}/^{238}\text{U}$  isotopic ratio in samples incorporating a total of about 1 mg of U. AMS will be shown to be the only technique able to achieve such a sensitivity together with unparalleled suppression of molecular isobaric interferences for the detection of rare isotopes of elements with (quasi)stable isotopes many orders of magnitude more abundant, such as U.

Nevertheless, the measurement of  $^{238}\text{Pu}$  abundance is heavily suffering interference from the atomic isobar  $^{238}\text{U}$ , about seven orders of magnitude more abundant, and cannot be achieved by any mass spectrometric technique; on the other hand ultra-low activity AS can isolate this isotope, while alpha particles from the decay of  $^{239}\text{Pu}$  and  $^{240}\text{Pu}$  cannot be energetically resolved. Combination of the two techniques provides the determination of the abundances of the full suite of Pu isotopes. Moreover, AS plays an important role also for the calibration of the spikes used as carriers for the AMS measurements and as overall cross check of the employed methodologies. An important role in pursuing the goal of ultrasensitive detection of actinide isotopes is played by the sample preparation procedures, which has to be performed in a very clean environment with ultralow contamination. The procedure to be setup will be able to isolate the elements of interest and produce samples in the form suitable for both AS and AMS. In the first case very thin and uniform layers have to be achieved, while purification respect to elements which can produce molecular interferences is of paramount importance for AMS. Preliminary sampling and conditioning of a properly representative sample; uranium and plutonium are separated from the sample following a systematic chemical protocol of pre-enrichment/separation; fractions of U and Pu are purified from every possible element that could cause radiochemical interference to AS; fractions of U and Pu must be converted into useful chemical and physical-chemical forms (De Cesare, 2009; Quinto et al., 2009; Wilcken et al., 2007).

Finally, besides the application of the developed technique to the assessment of actinide contamination of the NPP site and plant, a more general objective is to provide an ultrasensitive diagnostic tool for a variety of applications to the national and international community. Applications range across a broad spectrum. Isotopes of plutonium are finding application in tracing the dispersal of releases from nuclear accidents and reprocessing operations, in studies of the biokinetics of the element in humans, and as a tracer of soil loss and sediment transport.  $^{236}\text{U}$  has also been used to track nuclear releases, but additionally has a role to play in nuclear safeguards and in determining the extent of environmental contamination in modern theaters of war due to the use of depleted uranium weaponry.

## 2.4 Alpha-spectroscopy and mass spectroscopy

$^{236}\text{U}$  and  $^{239}\text{Pu}$  are present in environmental samples at ultra trace levels ( $^{236}\text{U}$  concentration is quoted to be in the order of pg/kg or fg/kg and  $^{239}\text{Pu}$  around 100 pg/kg) and are long-lived radionuclides (Perelygin & Chuburkov, 1997).

If one considers alpha-spectroscopy for the detection of  $^{239}\text{Pu}$ , assuming an efficiency of 50 % and a counting time of one month, one gets 64 counts (with a statistical uncertainty of 12%) with a total activity of 50  $\mu\text{Bq}$ , which correspond to about 40 million atoms, or about 15 fg. In addition, alpha-particle counting is unable to resolve the two most important plutonium isotopes,  $^{239}\text{Pu}$  and  $^{240}\text{Pu}$ , because their alpha-particle energies differ by only 11 keV in 5.25 MeV. Hence, the information on their isotopic ratio readily difficult to extract.

The  $23 \cdot 10^6$  y half-life of  $^{236}\text{U}$  limits the utility of alpha-particle spectroscopy for this isotope. For the detection of such small amounts one can exploit the sensitivity of mass spectrometric techniques. Conventional Mass Spectrometry, CMS, methods give information on the  $^{240}\text{Pu}/^{239}\text{Pu}$  ratio, and potentially have higher sensitivity than alpha-particle counting with values as low as 1 fg, but are sensitive to molecular interferences. Both  $^{236}\text{U}$  and  $^{238}\text{U}$  isotopes have been measured using either Thermal Ionization (TI-MS) or Inductively Coupled Plasma (ICP-MS) positive ion sources. For plutonium isotopes, abundance sensitivity is not a problem due to the absence of a relatively intense beam of similar mass. Molecular interferences such as  $^{238}\text{UH}^-$ ,  $^{208}\text{Pb}^{31}\text{P}$ , etc. may be a problem (Fifield, 2008). For uranium, isotope variability both in the molecular ( $^{238}\text{UH}^-$ ) and in tail contributions of main beam of  $^{238}\text{U}$  limits the sensitivity of ICPMS to  $^{236}\text{U}/^{238}\text{U}$  ratios of  $\sim 10^{-7}$ . TIMS ion sources, on the other hand, produce both much lower molecular beams and much less beam tail and so a sensitivity of  $\sim 10^{-10}$  in the  $^{236}\text{U}/^{238}\text{U}$  ratio is reached.

So that, the measurements of these isotopic ratios requires the resolution of mass spectrometric techniques, but only AMS allows the sensitivity needed e.g.  $^{236}\text{U}/^{238}\text{U}$  ratios of  $\sim 10^{-13}$ , 0.1 fg of  $^{236}\text{U}$  with about 1 mg of U, as well as for the  $^{239}\text{Pu}$ .

Although AMS has advantages over the other techniques for  $^{239,240,242,244}\text{Pu}$ , there are two other isotopes,  $^{238}\text{Pu}$  and  $^{241}\text{Pu}$ , which are of interest in some applications. Since the concentration of  $^{238}\text{U}$  is seven orders of magnitude higher than that of  $^{238}\text{Pu}$ , no chemical procedure is efficient to separate uranium and plutonium fractions to allow the mass spectrometric measurement of  $^{238}\text{Pu}$ . So alpha-spectroscopy remains the only suitable technique for the measurement of  $^{238}\text{Pu}$  concentration. The  $\beta^-$  emitter  $^{241}\text{Pu}$  can be measured with either AMS or with liquid scintillation counting. Its short half-life of 14 years results, however, in higher sensitivity for the latter (Fifield, 2008).

## 2.5 AMS of actinides isotopes

Actinides AMS measurements were pioneered at the IsoTrace laboratory in Toronto (CA) (Zhao et al., 1994; 1997), where the  $^{236}\text{U}$  content in an U ore was determined using the 1.6 MV AMS system. Moreover, the relative abundances of Pu isotopes were measured at 1.25 MV. Then, at the Australian National University (AUS) (Fifield et al., 1996; 1997) the utilization of a higher terminal voltage (4 MV) allowed to improve the sensitivity of the method, both for the detection limit as the minimum detectable number of U atoms in the sample, and for the lower limit of isotopic ratio measurable in samples at high concentration. Similar detection system have been developed at the Vienna Environmental Research Accelerator (VERA - AU) (Steier et al., 2002), at the Lawrence Livermore National Laboratory (LLNL - USA) (Brown et al., 2004), at the Australian Nuclear Science and Technology Organisation (ANSTO - AUS) (Hotchkis, 2000), at much lower energies at the Eidgenössische Technische

Hochschule - ETH in Zurich (CH) (Wacker et al., 2005), at Munich facility (GE) (Wallner et al., 2000) and at the accelerator of Weizmann Institute, Israel (Berkovits et al., 2000). New AMS actinides line based on 1MV and 3 MV tandems have recently been and will be installed, respectively, in Seville (Spain) and in the Salento (Italy). In both cases, they will be upgraded to perform actinides AMS measurements, being the injection and the analyzing magnets overdimensioned.

Two recent review papers (Fifield, 2008; Steier et al., 2010) summarize the results obtained in the laboratories active in the fields of actinides AMS. Summarizing, the two systems aiming to the best isotopic ratio sensitivity (ANU and VERA) have shown that it is possible to reach a sensitivity of  $10^{-13}$  for  $^{236}\text{U}$  in samples including about 1 mg of U. The ANSTO and LLNL laboratories quote a sensitivity respectively of about  $10^{-8}$  and  $10^{-9}$  with U amounts of the order of 1 ng. In the case of plutonium, there is no stable abundance isotopes available; the plutonium isotopic ratio is not a problem and a  $^{239}\text{Pu}$  concentration background of about 0.1 fg ( $2.5 \times 10^5$  atoms) is achieved, limited by the process blank count rate. In both cases these limits surmount by several orders of magnitude alpha spectrometry and conventional mass spectrometry. In nature, U stable abundant isotopes exist. For that reason, the sensitivity limit for the isotopic ratio depends on the U concentration in the sample. Thus, the AMS task is, for environmental samples, to push the sensitivity in the isotopic ratio measurement down to natural abundances ( $^{236}\text{U}/^{238}\text{U} \sim 10^{-9}$ - $10^{-13}$ ) in samples with sizeable amounts of U ( $\sim 1$  mg). On the other hand, for anthropogenically influenced samples, the required sensitivity for the measurement of the isotopic composition is alleviated, but significantly smaller amounts of U have to be used (down to 1 ng). For Pu, where no stable isotope interferences are present, the goal is the maximum possible detection efficiency, allowing few hundred counts from less than 1 million atoms in the sample.

The CIRCE laboratory is one of the few systems in the world able to perform such a measurement (De Cesare et al., 2010a) and the only one in Italy. Moreover it is 1 order of magnitude higher (De Cesare et al., 2010b) with respect to the 2 systems (ANU and VERA) providing the best  $^{236}\text{U}/^{238}\text{U}$  isotopic ratio sensitivity of  $10^{-13}$ , in samples including about 1 mg of U; it has low uranium contamination background, less than  $0.4 \mu\text{g}$  of  $^{236}\text{U}$  (De Cesare et al., 2011). The CIRCE actinides group aims to reach and to exceed the isotopic ratio sensitivity goal with the upgrade: the utilization of a TOF system and, in case, the installation of a magnetic quadrupole doublet. Regarding the Plutonium background results, the CIRCE is one of the best systems in the world (De Cesare, 2009).

### 3. AMS facilities

In this paragraph the facilities where the author was mainly involved will be illustrated: CIRCE and ANU AMS systems.

#### 3.1 CIRCE system

CIRCE is a dedicated AMS facility based on a 3MV-tandem accelerator (Terrasi et al., 2007). In contrast to many nuclear physics applications, the pre-treated sample material (a few mg is pressed into a 1 mm diameter Al cathodes and put in the ion source) itself is analyzed by two mass spectrometers which are coupled to the tandem accelerator. A schematic layout of the CIRCE facility is shown in Fig. 1.

The caesium sputter ion source is a 40-sample MC-SNICS (Multi Cathode Source for Negative Ions by Cesium Sputtering). A total injection energy of 50 keV is used; 50-300 nA  $^{238}\text{U}^{16}\text{O}^-$  molecules are energy selected by a spherical electrostatic analyzer (nominal bending radius



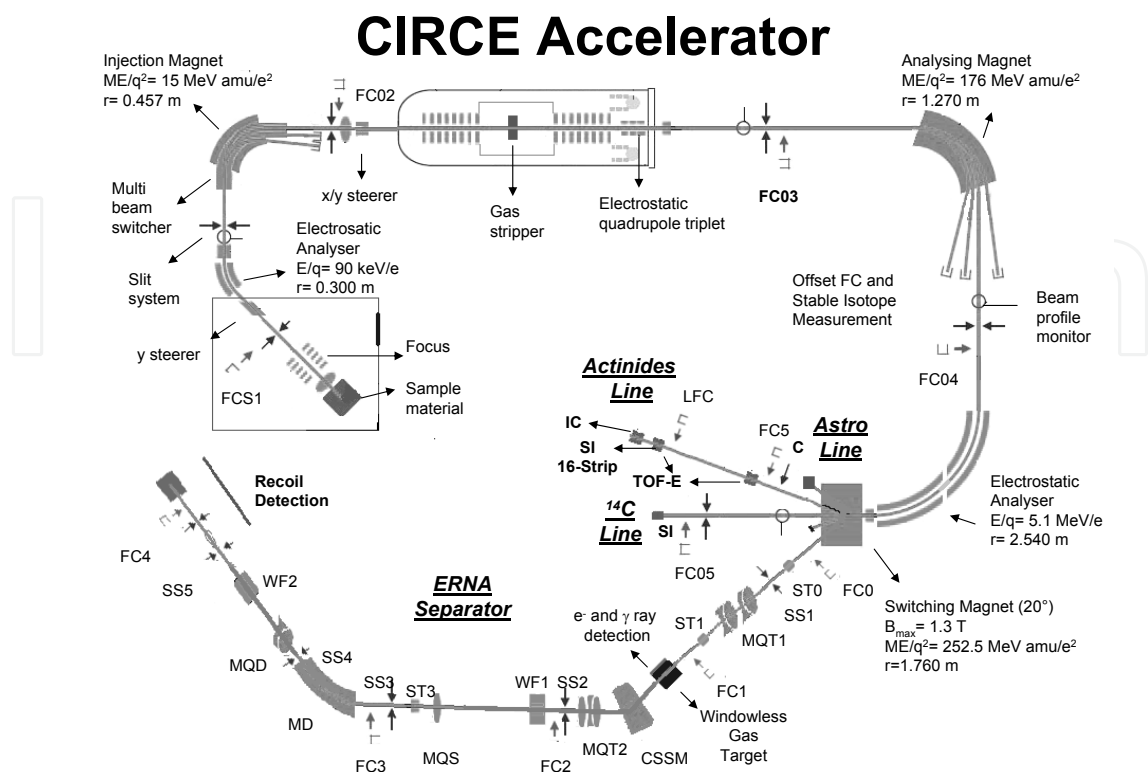


Fig. 1. Schematic layout of the CIRCE accelerator and of CIRCE accelerator upgrade with the actinides line and also the ERNA separator line, Astro line, besides the  $^{14}\text{C}$  original line: the switching magnet already inserted and the start and the stop TOF-E detector not yet inserted. FC denotes Faraday Cup (LFC in the actinides line is Last Faraday Cup), C denotes the Collimator in the heavy isotope line and the arrows indicate a slit system. ERNA is the acronym of European Recoil separator for Nuclear Astrophysics.

$r = 30$  cm, plate gap = 5 cm) which cuts the sputter low energy tail of the beam, with a bending angle of  $\pm 45^\circ$  and it is operated up to  $\pm 15$  kV. The maximum electric field strength is 6 kV/cm, resulting in an energy/charge state ratio of 90 keV/q. The  $90^\circ$  double focusing Low Energy (LE) injection magnet ( $r = 0.457$  m, vacuum gap = 48 mm,  $ME/q^2 = 15 \text{ MeV} \cdot \text{amu}/e^2$ ) allows high resolution mass analysis for all stable isotopes in the periodic table, mass resolution is  $M/\Delta M \sim 500$  with the object and image slits set to  $\pm 1$  mm, (De Cesare et al., 2010a). The insulated stainless steel chamber (MBS) can be biased from 0 kV to +15 kV for beam sequencing (e.g. between  $^{238}\text{U}^{16}\text{O}^-$ ,  $^{236}\text{U}^{16}\text{O}^-$  and between  $^{239}\text{Pu}^{16}\text{O}^-$ ,  $^{240}\text{Pu}^{16}\text{O}^-$ ,  $^{242}\text{Pu}^{16}\text{O}^-$ ).

The accelerator is contained inside a vessel filled with sulphur hexafluoride ( $\text{SF}_6$ ) at a pressure of about 6 bar. Two charging chains supply a total charging current to the terminal; about  $100 \mu\text{A}$  are delivered to the terminal for operation at 3.000 MV. Stabilization is achieved by GVM feedback on the charging system high voltage supply; the long term stability is about 1 kV peak-to-peak. At the terminal the ions lose electrons in the gas stripper, where Ar is recirculated by two turbo-pumps. The working pressure is about 1.3 mTorr for  $^{238}\text{U}^{5+}$  at 2.875 MV.

The ions with positive charge states are accelerated a second time by the same potential. The High Energy (HE) magnet, efficiently removes molecular break-up products (De Cesare et al., 2010a;b). The double focusing  $90^\circ$  HE bending magnet has  $r = 1.27$  m,  $ME/q^2 = 176$  MeV·amu/ $e^2$  and  $M/\Delta M = 725$ , with slit opening of  $\pm 1$  mm both at object and image points. The two  $45^\circ$  electrostatic spherical analyzers ( $r = 2.54$  m and gap = 3 cm) are operated up to  $\pm 60$  kV; energy resolution is  $E/\Delta E = 700$  for typical beam size. A switching magnet ( $B_{max} = 1.3$  T,  $r = 1.760$  m and  $ME/q^2 = 252.5$  MeV·amu/ $e^2$  at the  $20^\circ$  exit) is positioned after the ESA. Finally the selected ions are counted in an appropriate particle detector, either a surface barrier detector or a telescopic ionization chamber. The control of the entire system, is handled by the AccelNet computer based system via CAMAC interfaces or Ethernet, and the acquisition system is either AccelNet itself or FAIR (Fast Intercrate Readout) system, (Ordine et al., 1998).

### 3.1.1 CIRCE actinides measurement procedures

In this paragraph a description of the various steps of the  $^{236}\text{U}$  and  $^x\text{Pu}$  isotopes measurement are given. The relative abundance of  $^{238}\text{U}$  in environmental samples is several order of magnitude (up to 13) larger than the  $^{236}\text{U}$ . For this reason, while the number of events of  $^{236}\text{U}$  are measured in the final detector,  $^{238}\text{U}$  is measured as current in the high energy side. For the  $^x\text{Pu}$  isotopes, since no natural and so abundant isotopes exist, they are all measure in the final detector. Before performing measurements of samples, a tuning of the transport elements up to the final detector is made by setting the accelerator parameters to the detection of  $^{238}\text{U}$ . Then the MBS, the TV and the high energy ESA are scaled to select the rare isotopes. The sample preparation provides material that is sputtered as  $^x\text{U}^y\text{O}^-$  and  $^z\text{Pu}^w\text{O}^-$ . The negative molecular ions, ex.  $^{238}\text{U}^{16}\text{O}^-$ , are accelerated to an injection energy of  $E_{inj} = 50$  keV. To select different masses without changing the magnetic field, the energy of the ions inside the injection magnet is varied by applying an additional accelerating voltage to the bouncing system. The injected  $^{238}\text{U}^{16}\text{O}^-$  ions are accelerated by the positive high voltage towards the stripper, where they loose electrons and gain high positive charge states. The positive ions are, then, accelerated a second time by the same potential in the high energy tube of the tandem. This for  $^{238}\text{U}^{5+}$  results in an energy of  $E = 17.3$  MeV with a terminal voltage of  $V = 2.900$  MV. Ar is recirculated in the terminal stripper by two turbo-pumps; the working pressure is about 1.3 mTorr for  $^{238}\text{U}^{5+}$  at 2.875 MV (De Cesare et al., 2010b) and the stripping yield achieved for  $^{238}\text{U}^{5+}$  achieved is around 3.1%.

Molecular break-up products with mass over charge ratio ( $M/q$ ) different from that of the wanted ion, are removed by the combination of the high energy (HE) magnet and an electrostatic analyzer (ESA) whose object point is the image point of the analyzing magnet. For heavy ion measurements, the object and image slits of the injection magnet are closed to  $\pm 1$  mm, the slits of the analyzing magnet are closed to  $\pm 2$  mm and a collimator of 4 mm diameter is positioned in the beam waist at the  $20^\circ$  beam line.

The tuning procedure at CIRCE is made by the optimization of HE magnet and ESA in the high-energy side: they are optimized by maximizing the  $^{238}\text{U}^{5+}$  current in the Last Faraday Cup (LFC). The transmission efficiency between the HE magnet and LFC at  $20^\circ$  is 80 %, with the 4 mm collimator in.

Once the setup for the pilot beam  $^{238}\text{U}^{5+}$  is found, the voltage at the chamber of the injection magnet, the terminal voltage and the voltage of the ESA are scaled to transmit  $^{236}\text{U}^{5+}$ . In order to measure the  $^{236}\text{U}/^{238}\text{U}$  ratio, the measurement procedure is composed of three automatic steps:

1. measurement of  $^{238}\text{U}^{5+}$  current at the high energy side in FC04.
2. the voltage on the magnet vacuum chamber, the terminal voltage and the ESA are then scaled to transmit  $^{236}\text{UO}^-$  and a measurement of the count rate of  $^{236}\text{U}^{5+}$  in the detector is performed.
3. repetition of step 1

Steps 1 and 3 are necessary to estimate, by linear interpolation, the value of  $^{238}\text{U}^{5+}$  current at high energy side which would be measured simultaneously with  $^{236}\text{U}^{5+}$  counting.

In order to measure the  $^x\text{Pu}$  isotope ratios, the measurement procedure is composed of automatic steps:

1. tune the beam with the  $^{238}\text{U}^{5+}$  current up to LFC.
2. the voltage on the magnet vacuum chamber, the terminal voltage and the ESA are then scaled to transmit  $^x\text{PuO}^-$  and a measurement of the count rate of  $^x\text{Pu}^{5+}$  in the detector is performed.
3. repetition of step 2 for all the plutonium isotopes are needed (ex.  $^{242}\text{Pu}^{5+}$  spike for 18 s,  $^{240}\text{Pu}^{5+}$  for 60 s and  $^{239}\text{Pu}^{5+}$  for 30 s).
4. repetition of step 3 for 3 times.

### 3.1.2 CIRCE actinide results

Before the installation of a dedicated actinides beam line at CIRCE, preliminary results for the  $^{236}\text{U}/^{238}\text{U}$  background ratio level at  $0^\circ$  line, routinely used for  $^{14}\text{C}$  measurements, was of the order of  $1 \cdot 10^{-9}$  (De Cesare et al., 2010a). The measurement was obtained with the "K. k. Uranfabrik Joachimisthal" sample, the VERA in-house U standard,  $(6.98 \pm 0.32) \times 10^{-11}$  (Steier et al., 2008).

The main upgrade so far has been the addition of a switching magnet placed 50 cm after the exit of the high-energy ESA. The position of the magnet was decided by means of COSY infinity (Makino & Berz, 1999) magnetic optics simulation (De Cesare et al., 2010a), Fig. 2. This magnet provides a supplementary dispersive analyzing tool.

The abundance sensitivity results, using a 16-strip silicon detector, have shown that, in the upgraded CIRCE heavy ions beamline after the switching magnet installation, a background level  $< 5.6 \times 10^{-11}$  has been reached, Fig. 3, compared to  $3.0 \times 10^{-9}$  obtained previously (De Cesare et al., 2010b; Guan, 2010).

Although most of the  $^{238}\text{U}$  are suppressed at the injector side, by the analyzing magnet and electrostatic analyzer, a small fraction of this intense beam can still interfere with the  $^{236}\text{U}$  measurement. The main reasons for this "leakage" of interfering ions are charge exchange processes due to residual gas in the system. Scattering on the residual gas, electrodes, slits or vacuum chamber walls can also allow the background to pass a filter. However, the scattering cross-section is in the order of  $10^{-20} \text{ cm}^2$  whereas the cross section of charge changing is  $10^{-16}$ - $10^{-15} \text{ cm}^2$  (Betz, 1972; Vockenhuber et al., 2002).

Moreover, in the upgraded CIRCE heavy ions beamline, after the TOF-E installation, a background level of about  $2.9 \times 10^{-11}$ , summing over the central six strips, has been reached, compared to  $\sim 5.6 \times 10^{-11}$  obtained with a 16 strip silicon detector alone. This small background reduction is attributed to the 1.6 ns time resolution mainly due to the thickness of the  $4 \mu\text{g}/\text{cm}^2$  LPA (Maier-Komor et al., 1997; 1999) carbon foil, (De Cesare, 2009).

The CIRCE laboratory is not so far from the two systems (ANU and VERA) that provide the best  $^{236}\text{U}/^{238}\text{U}$  isotopic ratio sensitivity of  $10^{-13}$ , in samples including about 1 mg of U.

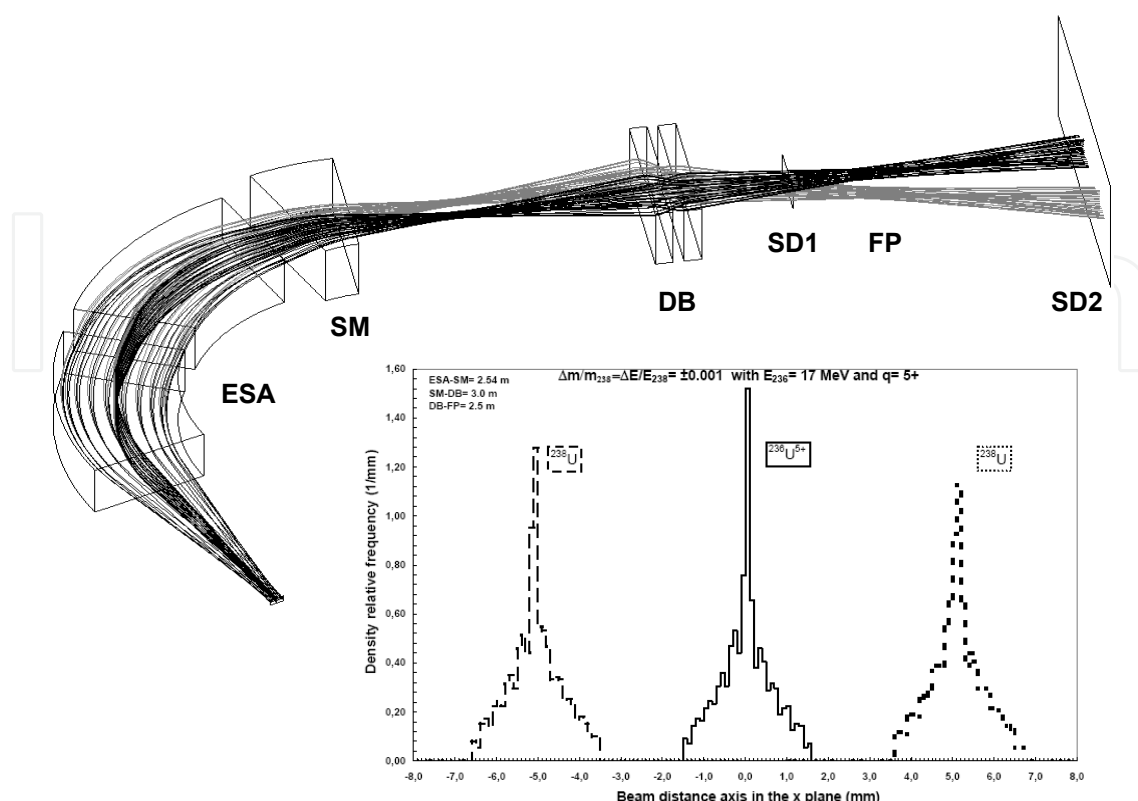


Fig. 2. The COSY infinity magnetic optics simulation is shown, where the development of two beams has been analyzed, starting from the waist of the high-energy magnet with a relative energy difference of  $\Delta E/E = 0.001$  (corresponds to the resolution of the ESA). The adopted beam profiles are approximately Gaussian, with a halfwidth of 0.15 cm. A maximum divergence of 3 mrad was assumed. Simulations were performed for different geometric configurations. The distance ESA-SM (energy electrostatic analyzer-switching magnet), SM-DB (switching magnet-magnetic quadrupole doublet) and DB-FP (Focal Plane = the doublet focusing position) are shown in the upper part. The density relative frequency in function of beam distance in the x-plane is shown in the lower part. The central (solid line) peak is  $^{236}\text{U}^{5+}$  and the dashed and dotted are the  $^{238}\text{U}$  beams in the two opposite x positions, where the dashed one is not shown in the simulation

An overview of the planned upgrade of the CIRCE system using a TOF-E system, with a flight path of 3 m and a thinner DLC carbon foil,  $0.6 \mu\text{g}/\text{cm}^2$  is described in (De Cesare, 2009).

Regarding the concentration sensitivity results, a  $4 \mu\text{g}$  uranium concentration sensitivity has been reached using only with the 16 strip silicon detector. That correspond to about 40 fg of  $^{236}\text{U}$  and  $10^8$   $^{236}\text{U}$  atoms for a sample with isotopic ratio of  $10^{-8}$  (De Cesare et al., 2011).

For the  $^{239}\text{Pu}$  concentration sensitivity results, the uranium background corresponding to the  $^{239}\text{Pu}$  settings is at the level of 1 ppb. This is to be compared with the 10 ppm of ANSTO and 100 ppb of ANU. The CIRCE Lab. has at present a  $^{239}\text{Pu}$  sensitivity level less than 0.1 fg, since 500 ng of uranium is required to produce an apparent  $^{239}\text{Pu}$  concentration of 0.1 fg (De Cesare et al., 2011); for the Pu background level, CIRCE is one of the best system in the word.

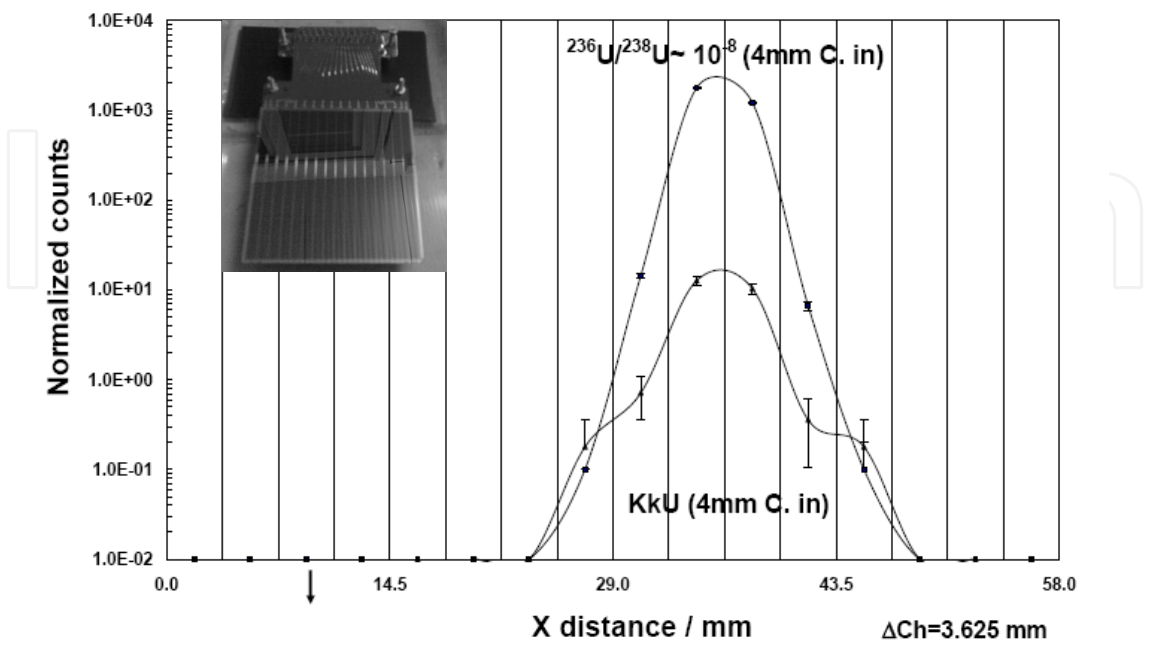


Fig. 3. Normalized counts (counts in the detector in 300 s over FC04 current corrected for the transmission  $\sim 80\%$  between FC04 and LFC) versus horizontal position of the 16-strip silicon detector.  $\text{Ch} = 3.625\text{ mm}$  is the distance between the center of two adjacent strips. A photo of the 16-strip detector is also shown. The bigger peak represents the position on the detector of the  $^{236}\text{U}$  obtained with a spike sample; the nominal ratio is  $^{236}\text{U}/^{238}\text{U} \sim 10^{-8}$ . The lower  $^{236}\text{U}$  peak is obtained with the KkU VERA in house U standard, see text. The arrow indicates that the normalized counts at that position are lower than  $1 \times 10^{-2}$  counts/nA.

3.2 ANU system

The ANU AMS system is based on a 15MV-tandem accelerator (Fifield et al., 1996). The high terminal voltage is required to apply certain techniques of isobar separation effectively, this makes the ANU tandem the best suited accelerator for the heavier isotopes e.g.,  $^{36}\text{Cl}$  and  $^{53}\text{Mn}$  (Winkler, 2008). When the lower energy is necessary, for  $^{236}\text{U}$  and  $^x\text{Pu}$  isotopes, sections of the accelerator tube are shorted out, in order to optimize the ion optics for maximum transmission.

The pre-treated sample material (a few mg is pressed into a 1 mm diameter Al cathode and put in the ion source) itself is analyzed by two mass spectrometers which are coupled to the tandem accelerator. A schematic layout of the ANU 15 MV tandem facility is shown in Fig. 4. The caesium sputter ion source is a 32-sample MC-SNICS. This multi-cathode arrangement allows for measuring many samples without opening the source or employing a more complicated single cathode exchange mechanism. A total injection energy of 100 keV was used and  $\sim 20\text{ nA}$  of  $^{238}\text{U}^{16}\text{O}^-$  molecular ions are mass rigidity selected by the  $90^\circ$  double focusing Low Energy (LE) injection magnet ( $r = 0.83\text{ m}$ ,  $B_{\text{max}} = 1.3\text{ T}$ ,  $\text{ME}/q^2 \simeq 56\text{ MeV}\cdot\text{amu}/e^2$ ). This allows high resolution mass analysis for all stable isotopes in the periodic table. In contrast to the CIRCE system, there is no electrostatic analyzer, and hence the



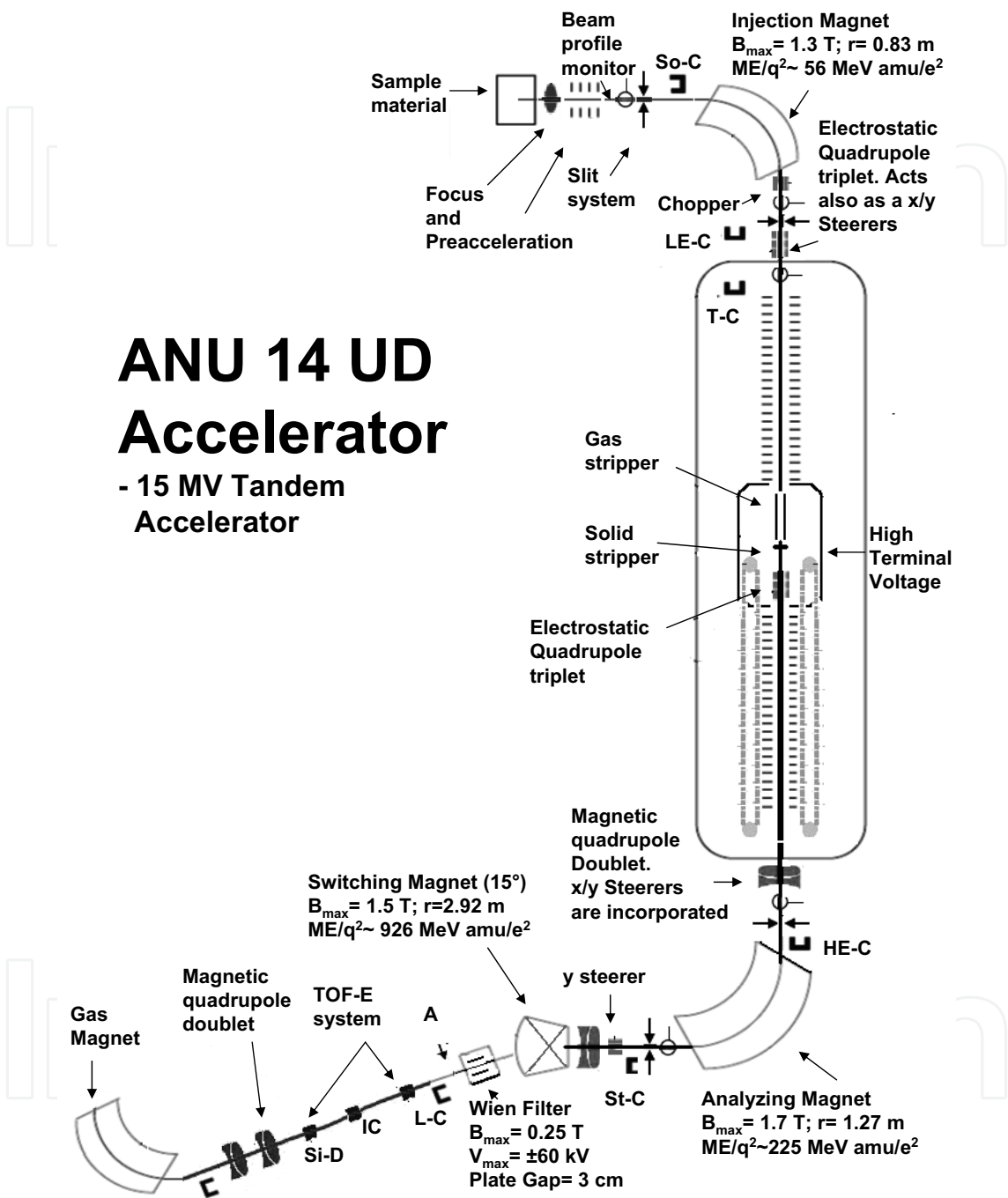


Fig. 4. Schematic lay out of the 15 MV ANU 14-UD (Units Doubled) Accelerator and the  $^{236}\text{U}$  and  $^x\text{Pu}$  isotopes detection line. The Switching Magnet, the Wien Filter, the start and the stop TOF-E detector, the Ionization Chamber, the magnetic quadrupole doublet and the Gas Magnet are shown in the line. C denotes the position-Faraday Cup, A denotes the Aperture of  $1.5 \times 4.0 \text{ mm}^2$  and the arrows indicate a slits system. The Accelerator is vertical up to the switching magnet that is indicate with a cross.

low-energy sputter tail is not removed prior to injection into the accelerator. For this reason, it is preferred to tune the system with  $^{232}\text{Th}^{16}\text{O}^-$  rather than  $^{238}\text{U}^{16}\text{O}^-$  (see next section).

A beam profile monitor (BPM) before the magnet and Faraday cups after the magnet (LE-Cup and Tank-Cup) are used to monitor the beam during the tuning. The injection beam line also features an electrostatic chopper that allows to reduce the beam intensity in cases where the beam currents are too high for injection into the tandem accelerator or counting rates that would be too high for the detector (e.g.  $^{234}\text{U}$ ). An electrostatic quadrupole and steerers are available to have the ions pass on an optimum trajectory for injection into the accelerator.

The terminal is charged by chains made of metal pellets which are isolated from each other by nylon links. The pellets supply a total charging current to the terminal of about  $230\ \mu\text{A}$ . The accelerator is contained inside a vessel filled with sulphur hexafluoride ( $\text{SF}_6$ ) at a pressure of about 6 bar. The voltage is measured by a generating voltmeter. Regulation is achieved by employing a controlled corona discharge from ground to terminal. Both a gas stripper and a foil stripper are available at the terminal. At the terminal the ions lose electrons in the stripper, where  $\text{O}_2$  is recirculated by two turbo-pumps; the working pressure is about 1 mTorr for  $^{238}\text{U}^{5+}$  at 3.995 MV. Molecular ions are dissociated and the now atomic ions stripped to higher positive charge states (Litherland, 1980). The choice of charge state for heavy ions depends critically on a compromise between its stripping yield and the capability of the subsequent analyzing magnet to bend such ions. At  $\sim 4\ \text{MV}$ ,  $\text{ME}/q^2$  is  $\sim 226\ \text{MeV}\cdot\text{amu}/e^2$  for  $^{238}\text{U}^{5+}$  and  $\text{ME}/q^2$  is  $\sim 293\ \text{MeV}\cdot\text{amu}/e^2$  for  $^{238}\text{U}^{4+}$ ; since the double focusing HE magnet reaches a maximal  $\text{ME}/q^2 \sim 225\ \text{MeV}\cdot\text{amu}/e^2$ , the  $5+$  represents the lowest charge state which can be bent by the HE magnet. Although the stripping yield to  $4+$  charge state is higher than  $5+$ , it would be necessary to operate at lower terminal voltage in order to bend the ions. Since the transmission (due to the larger scattering angle) and the energy of the ions at this voltage is lower there is no gain to use the lower charge state.

The ions with positive charge states are accelerated a second time by the same potential. The High Energy (HE) magnet, efficiently removes molecular break-up products. The double focusing  $90^\circ$  HE bending magnet has  $r = 1.27\ \text{m}$ ,  $B_{\text{max}} = 1.7\ \text{T}$ ,  $\text{ME}/q^2 \simeq 225\ \text{MeV}\cdot\text{amu}/e^2$ . A switching magnet ( $B_{\text{max}} = 1.5\ \text{T}$ ,  $r = 2.92\ \text{m}$  and  $\text{ME}/q^2 \simeq 926\ \text{MeV}\cdot\text{amu}/e^2$  at the  $15^\circ$  exit) is positioned after the HE magnet. A Wien filter ( $B_{\text{max}} = 0.25\ \text{T}$ ,  $V_{\text{max}} = \pm 60\ \text{kV}$  with a Plate Gap =  $3\ \text{cm}$ ) is employed to remove backgrounds.

Finally the selected ions are counted in a final detector. The control of the acquisition system is handled via Ethernet interfaces.

### 3.2.1 ANU actinides measurement procedures

In this paragraph a description of the various steps of the  $^{236}\text{U}$  and  $^x\text{Pu}$  isotope measurements will be given. The relative abundance of  $^{238}\text{U}$  in environmental samples is many orders of magnitude (up to 13) larger than the  $^{236}\text{U}$ . For this reason, while the number of events of  $^{236}\text{U}$  are measured in the final detector,  $^{238}\text{U}$  is measured as a current at the high energy side. Before performing measurements of samples, a tuning of the transport elements up to the final detector is required in order to maximize the ion optical transmission. The tuning is made by setting the parameters of the beam line to the detection of  $^{232}\text{Th}$ . In order to have a good negative ion yield, molecular negative ions  $^{232}\text{Th}^{16}\text{O}^-$  are extracted from the ion source. The negative molecular ions,  $^{232}\text{Th}^{16}\text{O}^-$ , are accelerated to injection energy of  $E_{\text{inj}} = 100\ \text{keV}$ .

The injected ions are accelerated by the positive high voltage towards the gas stripper, where they lose electrons and gain high positive charge states. The positive ions are then accelerated a second time by the same potential in the high energy tube of the tandem. For  $^{232}\text{Th}^{5+}$ ,

this results in an energy of  $E = 24.424$  MeV with a terminal voltage of  $V = 4.098$  MV. The stripping yield is the ratio between the  $^{232}\text{Th}^{5+}$  beam current at the Faraday cup after the analyzing magnet (St-C) divided by 5 and the  $^{232}\text{Th}^{16}\text{O}^-$  current measured at the entrance to the accelerator (T-C), and is about 3%. Molecular break-up products with mass over charge ratio  $M/q$  different from that of the wanted ion are removed by the analyzing magnet and switching magnet. The Wien filter is employed to remove backgrounds which have the same  $ME/q^2$  as the ions of interest but different velocities in the actinides line. For heavy ion tuning, the object and image slits of the injection magnet are closed to  $\pm 1$  mm, the slits of the analyzing magnet are closed to  $\pm 1.25$  mm and an aperture of  $1.5 \times 4.0$  mm<sup>2</sup> is used if high selectivity is required just after the Wien filter. For actual measurements, the object and image slits of the injection magnet are opened to  $\pm 2$  mm, the slits of the analyzing magnet are opened to  $\pm 3$  mm and the aperture is out.

For Uranium measurements, once the setup for the pilot beam  $^{232}\text{Th}^{5+}$  is found, the fields of the injection magnet, the terminal voltage of the accelerator and the electric field of the Wien filter are scaled to  $^{238}\text{U}^{5+}$  for a fine tuning and then to the other wanted masses. For  $^{236}\text{U}/^{238}\text{U}$ , the measurement procedure is composed of two loops of three steps. Each loop consists of integration of the  $^{238}\text{U}^{5+}$  beam current for 10 s in the L-C, counting of  $^{236}\text{U}^{5+}$  ions for 5 min in the TOF-E system and a final  $^{238}\text{U}^{5+}$  integration. For  $^{233}\text{U}$  (tracer),  $^{234}\text{U}$  and  $^{236}\text{U}$ , the measurement procedure is composed of two loops of four steps. The isotope sequence would usually start with the reference isotope  $^{233}\text{U}$  followed by  $^{234}\text{U}$  and  $^{236}\text{U}$ , and finishing with  $^{233}\text{U}$ . All of them are counted with the TOF-E system. The typical counting intervals were 1 minute for  $^{233}\text{U}$ , 1 minute for  $^{234}\text{U}$  and 5 minutes for  $^{236}\text{U}$ .

For Plutonium measurements, once the setup for the pilot beam  $^{232}\text{Th}^{5+}$  is found, since  $^{238}\text{U}^{5+}$  may cause interference for  $^{239}\text{Pu}^{5+}$ , the fields of the injection magnet, the terminal voltage of the accelerator and the electric field of the Wien filter are scaled to the Pu wanted masses,  $^{239}\text{Pu}$ ,  $^{240}\text{Pu}$  and  $^{242}\text{Pu}$  (tracer). The measurement procedure is composed of two loops of four steps; the isotope sequence would usually start with the reference isotope  $^{242}\text{Pu}$  followed by  $^{240}\text{Pu}$  and  $^{239}\text{Pu}$ , and finishing with  $^{242}\text{Pu}$ . All of them are counted with a multiple electrode ionization chamber that is routinely used for measurements of  $^x\text{Pu}$  isotopes. The typical counting intervals were 1 minute for  $^{242}\text{Pu}$ , 5 minutes for  $^{240}\text{Pu}$  and 3 minutes for  $^{239}\text{Pu}$ .

### 3.2.2 Detection systems and ANU actinide results

Although most of the  $^{238}\text{U}$  are suppressed at the injector side and by the analyzing magnet and Wien filter, a small fraction of this intense beam can interfere with the  $^{236}\text{U}$  measurement even if the expected separation in the ion-optical filters is large, paragraph 3.1.2. For this reason the detection of the  $^{236}\text{U}$  at ANU is made with a TOF-E detection. The configuration of the TOF detection system is as follows (Wilcken, 2006; Winkler, 2008); the start detector assembly is based on a MCP and a foil is placed at an angle of  $45^\circ$  to the beam. The MCP detects the backscattered electrons from a  $0.6 \mu\text{g}/\text{cm}^2$  thick diamond-like carbon (DLC) (Liechtenstein et al., 1999; 2002; 2004; 2006) foil that is used in the start detector to minimize scattering. The stop detector is a  $200 \text{ mm}^2$  silicon surface barrier detector which also provides a total energy signal. The foils are mounted on a Cu mesh with a transparency of  $\sim 75\%$ . The MCP detector was operated with the anode at ground, the accelerating grid and the front face of the MCP at  $-1.8$  kV, and the carbon foil at  $-2.8$  kV. The presence of the foil, which is oriented at  $45^\circ$  to the beam, has two important consequences for the system. First, it causes scattering, which if through a large-enough angle can cause ions to miss the stop detector. This can be minimized by using the thinnest possible foil. Secondly, the  $45^\circ$  tilt introduces differences in path length

and therefore also in flight time due to the finite size of the beam at the start detector. The effect of the flight path variations on the resolution of the system is minimized by using an aperture that is 3.5 mm wide in the horizontal plane. This is attached on top of the grid-foil assembly.

For plutonium measurements no interfering ions exist; an ionization chamber is suitable for such a detection. The ANU configuration of the ionization chamber (Fifield et al., 1996; Wilcken, 2006; Wilcken et al., 2008) are the following;  $\sim 50$  torr of propane is used as the detector gas and the window is a  $0.7 \mu\text{m}$  thick Mylar foil. Applied voltages are: cathode  $\simeq -600$  V, detector window  $\simeq -300$  V, first grid at ground, second grid at  $\simeq +200$  V and anode  $\simeq +600$  V. The energy of the  $^{239}\text{Pu}^{5+}$  ions is  $\sim 24.5$  MeV. At this energy, the range of the plutonium ions in the ANU detector is  $\sim 35$  mm, which is roughly 18% of the length of the detector. The energy loss and straggling in the detector window are approximately 4.5 MeV and 450 keV, respectively. In addition, according to the manufacturer, a typical value for the surface roughness of the Mylar window is 38 nm, which is 5% of the thickness of the window and contributes an additional 140 keV of straggling. All of these result in an energy resolution of  $\sim 4\%$ .

Regarding the abundance sensitivity results, the ANU is the best system in the world together with VERA laboratory (Steier et al., 2010). The ANU is able to obtain values of  $^{236}\text{U}/^{238}\text{U} \simeq 10^{-13}$  (Wilcken et al., 2008), in samples including about 1 mg of U. This results is obtained with a time of flight of 2.3 m.

Preliminary results have been obtained with a 6 m flight path; the longer flight path confers a substantial improvement in the ability to separate  $^{235}\text{U}$  and  $^{236}\text{U}$  with little reduction in efficiency (Fifield, 2011).

The concentration sensitivity limit is of the order of  $\sim 1 \mu\text{g}$  of uranium.

As regard the  $^{239}\text{Pu}$  concentration sensitivity results, the uranium background at the  $^{239}\text{Pu}$  settings is at the level of 100 ppb of the uranium concentration, i.e. 1 ng of uranium in the sample results in a background equivalent to 0.1 fg of  $^{239}\text{Pu}$  (Fifield, 2008).

#### 4. Summary and conclusion

The actinides detection technique described in this chapter can be applied in the assessment of contaminations from nuclear facility and used as sensitive fingerprints of programmed and accidental releases; a more general goal of this technique is to provide an ultrasensitive diagnostic tool for a variety of applications to the international community. Moreover the origin of actinides are discussed as well as the potential of actinides to serve as a tracer for geomorphologic processes.

The sensitivity of the different actinides measurements method and the peculiarity of the AMS technique with respect to AS and CMS techniques have been illustrated. Furthermore the principles and methodology of heavy-element AMS as applied to U and Pu isotopes, and the ways in which these have been implemented in various laboratories around the world, have been discussed. In particular the measurement procedures and the concentration and abundance sensitivity results of two systems, CIRCE and ANU, have been described in more details.

Those are two of the few systems in the world able to perform such measurements; the CIRCE is the only one in Italy.

The CIRCE system is at level of  $\sim 10^{-12}$   $^{236}\text{U}/^{238}\text{U}$  isotopic ratio sensitivity which is still one order of magnitude higher than the ANU and VERA systems.

As future plan the CIRCE actinides group foresees to reach and exceed this sensitivity ratio goal with the new upgrade: the utilization of a TOF-E system with a thinner carbon foil and, if necessary, with a longer time of flight.

Regarding the Plutonium background results, the CIRCE is one of the best systems in the world; it is at the level of 1 ppb. This is to be compared with ANSTO where the uranium background is at the level of 10 ppm, and the ANU system where it is at the level of 100 ppb. The CIRCE laboratory has at present a  $^{239}\text{Pu}$  sensitivity level less than 0.1 fg.

## 5. Acknowledgment

I kindly thank Prof. F. Terrasi, A. D'Onofrio, N. De Cesare, L. Gialanella, Dr. C. Sabbarese from SUN and Prof. L. K. Fifield, Dr. S. G. Tims from ANU and Dr. Y-J Guan from Guangxi University of Nanning and all the CIRCE actinides group who helped me to make this work possible.

Dr. P. Steier from VERA and Dr. D. Rogalla from Ruhr-Universität of Bochum and Dr. A. Di Leva from University of Naples and Dr. A. M. Esposito from SoGIN, for useful discussions and suggestions. This work was supported by SoGIN, Società Gestione Impianti Nucleari.

## 6. References

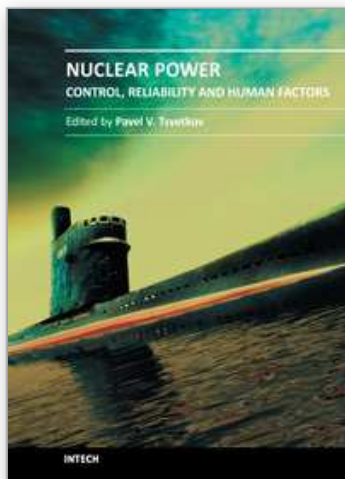
- Beasley, T.M.; Kelley, J.M.; Maiti, T.C.; Bond, L.A. (1998).  $^{237}\text{Np}/^{239}\text{Pu}$  Atom Ratios in Integrated Global Fallout: a Reassessment of the Production of  $^{237}\text{Np}$ . *Journal of Environmental Radioactivity*, Vol. 38, pp 133-146
- Berkovits, D.; Feldstein, H.; Ghelberg, S.; Hershkowitz, A.; Navon, E.; Paul, M. (2000).  $^{236}\text{U}$  in uranium minerals and standards. *Nuclear Instruments and Methods in Physics Research B*, Vol. 172, pp 372-376
- Betz, HD. (1972). Charge states and charge-changing cross sections of fast heavy ions penetrating through gaseous and solid media. *Reviews of Modern Physics*, Vol. 44, pp 465-539
- Brown, T.A.; Marchetti, A.A.; Martinelli, R.E.; Cox, C.C.; Knezovich, J.P.; Hamilton, T.F. (2004). Actinide measurements by accelerator mass spectrometry at Lawrence Livermore National Laboratory. *Nuclear Instruments and Methods in Physics Research B*, Vol. 223/224, pp 788-795
- Chiappini, R.; Pointurier, F.; Millies-Lacroix, J.C.; Lepetit, G.; Hemet, P. (1999).  $^{240}\text{Pu}/^{239}\text{Pu}$  isotopic ratios and  $^{239+240}\text{Pu}$  total measurements in surface and deep waters around Mururoa and Fangataufa atolls compared with Rangiroa atoll (French Polynesia). *The Science of the Total Environment*, Vol. 237/238, pp 269-276
- De Cesare, M. (2009). Accelerator Mass Spectrometry of actinides at CIRCE. *Phd Thesis*, Second University of Naples, Department of Environmental Science, Caserta (Italy)
- De Cesare, M.; Gialanella, L.; Rogalla, D.; Petraglia, A.; Guan, Y.; De Cesare, N.; D'Onofrio, A.; Quinto, F.; Roca, V.; Sabbarese, C.; Terrasi, F. (2010). Actinides AMS at CIRCE in Caserta (Italy). *Nuclear Instruments and Methods in Physics Research B*, Vol. 268, pp 779-783
- De Cesare, M.; Guan, Y.; Quinto, F.; Sabbarese, C.; De Cesare, N.; D'Onofrio, A.; Gialanella, L.; Petraglia, A.; Roca, V.; Terrasi, F. (2010). Optimization of  $^{236}\text{U}$  AMS at CIRCE. *Radiocarbon*, Vol. 52, pp 286-294
- De Cesare, M.; Fifield, L.K.; Sabbarese, C.; Tims, S. G.; De Cesare, N.; D'Onofrio, A.; D'Arco, A.; Esposito, A. M.; Petraglia, A.; Roca, V.; Terrasi, F. (2011), AMS12 conference



- proceeding: Actinides AMS at CIRCE and  $^{236}\text{U}$  and Pu measurements of structural and environmental samples from in and around a mothballed nuclear power plant.
- Diamond, H.; Fields, P.R.; Stevens, C.S.; Studier, M.H.; Fried, S.M.; Inghram, M.G.; Hess, D.C.; Pyle, G.L.; Mech, J.F.; Manning W.M.; Ghiorso, A.; Thompson, S.G.; Higgins, G.H.; Seaborg G.T.; Browne, C.I.; Smith, H.L.; Spence, R. W. (1960). Heavy Isotope Abundances in Mike Thermonuclear Device. *Physical Review*, Vol. 119, 2000-2004
- Fifield, L.K.; Cresswell, R.G.; Tada, M.L.D.; Ophel, T.R.; Day, J.P.; Clacher, A.P.; King, S.J.; Priest, N.D. (1996). Accelerator mass spectrometry of plutonium isotopes. *Nuclear Instruments and Methods in Physics Research B*, Vol. 117, pp 295-303
- Fifield, L.K.; Clacher, A.P.; Morris, K.; King, S.J.; Cresswell, R.G.; Day, J.P.; Livens, F.R. (1997). Accelerator mass spectrometry of the planetary elements. *Nuclear Instruments and Methods in Physics Research B*, Vol. 123, pp 400-404
- Fifield L.K. (2008). Accelerator mass spectrometry of the actinides. *Quaternary Geochronology*, Vol. 3, pp 276-290
- Fifield, L.K.; Tims, S.G.; Stone, J.O.; Argento, D.C.; De Cesare, M. (2011), AMS12 conference proceeding: Ultra-sensitive measurements of  $^{36}\text{Cl}$  and  $^{236}\text{U}$  at the Australian National University
- Guan, Y.G.; De Cesare, M.; Terrasi, F.; Quinto, F.; Sabbarese, C.; De Cesare, N.; D'Onofrio, A.; Wang, H. J. (2010).  $^{236}\text{U}$  AMS measurement at CIRCE. *Chinese Physics C*, Vol. 34, pp 1729-1732
- Hotchkis, M.A.C.; Child, D.; Fink, D.; Jacobsen, G.E.; Lee, P.J.; Mino, N.; Smith, A.M.; Tuniz, C. (2000). Measurement of  $^{236}\text{U}$  in environmental media. *Nuclear Instruments and Methods in Physics Research B*, Vol. 172, pp 659-665
- Hrneceka, E.; Steier, P.; Wallnerbet, A. (2005). Determination of plutonium in environmental samples by AMS and alpha spectrometry. *Applied Radiation and Isotopes*, Vol. 63, pp 633-638
- Ketterer, M.E.; Hafer, K.M.; Link, C.L.; Royden, C.S.; Hartsock, W.J. (2003). Anthropogenic  $^{236}\text{U}$  at rocky flats, Ashtabula river harbor, and Mersey estuary: three case studies by sector inductively coupled plasma mass spectrometry. *Journal of Environmental Radioactivity*, Vol. 67, pp 191-206
- Ketterer, M. E. & Szechenyi, S.C. (2008). Determination of plutonium and other transuranic elements by inductively coupled plasma mass spectrometry: A historical perspective and new frontiers in the environmental sciences. *Spectrochimica Acta Part B*, Vol. 63, pp 719-737
- Koide, M.; Bertine, K.K.; Chow, T.J.; Goldberger, E.D. (1985). The  $^{240}\text{Pu}/^{239}\text{Pu}$  ratio, a potential geochronometer. *Earth and Planetary Science Letters*, Vol. 72, pp 1-8
- Liechtenstein, V.Kh.; Ivkova, T.M.; Olshanski, E.D.; Baranov, A.M.; Repnow, R.; Hellborg, R.; Weller, R.A.; Wirth, H.L. (1999). Preparation and comparative testing of advanced diamond-like carbon foils for tandem accelerators and time-of-flight spectrometers. *Nuclear Instruments and Methods in Physics Research A*, Vol. 438, pp 79-85
- Liechtenstein, V.Kh.; Ivkova, T.M.; Olshanski, E.D.; Repnow, R.; Levin, J.; Hellborg, R.; Persson, P.; Schenkel, T. (2002). Advances in targetry with thin diamond-like carbon foils. *Nuclear Instruments and Methods in Physics Research A*, Vol. 480, pp 185-190
- Liechtenstein, V.Kh.; Ivkova, T.M.; Olshanski, E.D.; Golser, R.; Kutschera, W.; Steier, P.; Vockenhuber, C.; Repnow, R.; von Hahn, R.; Friedrich, M.; Kreissig, U. (2004). Recent investigations and applications of thin diamond-like carbon (DLC) foils, *Nuclear Instruments and Methods in Physics Research A*, Vol. 521, pp 197-202

- Liechtenstein, V.Kh.; Ivkova, T.M.; Olshanski, E.D.; Repnow, R.; Steier, P.; Kutschera, W.; Wallner, A.; von Hahn, R. (2006). Preparation and investigation of ultra-thin diamond-like carbon (DLC) foils reinforced with collodion. *Nuclear Instruments and Methods in Physics Research A*, Vol. 561, pp 120-123
- Litherland A.E. (1980). Ultrasensitive Mass Spectrometry with Accelerators. *Annual Review of Nuclear and Particle Science*, Vol. 30, 437-473
- Maier-Komor, P.; Bergmaier, A.; Dollinger, G.; Frey, C.M.; Krner, H.J. (1997). Improvement of the preparation procedure of carbon stripper foils from the laser ablation-deposition process. *Nuclear Instruments and Methods in Physics Research A*, Vol. 397, pp 131-136
- Maier-Komor, P.; Dollinger, G.; Krner, H.J. (1999). Reproducibility and simplification of the preparation procedure for carbon stripper foils by laser plasma ablation deposition. *Nuclear Instruments and Methods in Physics Research A*, Vol. 438, pp 73-78
- Makino, Kyoko & Berz, Martin (1999). COSY INFINITY version 8. *Nuclear Instruments and Methods in Physics Research A*, Vol. 427, pp 338-343
- O'Donnell, R.G.; Mitchell, P.I.; Priest, N.D.; Strange, L.; Fox, A.; Henshaw, D.L.; Long, S.C.; (1997). Variations in the concentration of plutonium, strontium-90 and total alpha-emitters in human teeth collected within the British Isles. *Science of the Total Environment*, Vol. 201, pp 235-243
- Ordine, A.; Boiano, A.; Vardaci, E.; Zaghi, A.; Brondi, A. (1998). A new fast trigger and readout bus system. *Nuclear Science*, Vol. 45, pp 873-879
- Perelygin, V.P. & Chuburkov, Yu.T. (1997). Man-made plutonium<sup>239</sup> possible serious hazard for living species. *Radiation Measurements*, Vol 28, pp 385-392
- Quinto, F. (2007). Assessing radioactive contamination in the environment around the Garigliano Nuclear Power Plant. *Phd Thesis*, Second University of Naples, Department of Environmental Science, Caserta (Italy)
- Quinto, F.; Steier, P.; Wallner, G.; Wallner, A.; Srncik, M.; Bichler, M.; Kutschera, W.; Terrasi, F.; Petraglia, A.; Sabbarese, C. (2009). The first use of <sup>236</sup>U in the general environment and near a shutdown nuclear power plant. *Applied Radiation and Isotopes*, Vol. 67, pp 1775-1780
- Richter, S.; Alonso, A.; Bolle, W.D.; Wellum, R.; Taylor, P.D.P. (1999). Isotopic fingerprints for natural uranium ore samples. *International Journal of Mass Spectrometry*, Vol. 193, pp 9-14
- Roca, V.; Napolitano, M.; Speranza, P.R.; Gialanella, G. (1989). Analysis of radioactivity levels in soils and crops from the Campania region (South Italy) after the Chernobyl accident. *Journal of Environmental Radioactivity*, Vol. 9, pp 117-129
- Sakaguchi, A.; Kawai, K.; Steier, P.; Quinto, F.; Mino, K.; Tomita, J.; Hoshi, M.; Whitehead, N.; Yamamoto, M. (2009). First results on <sup>236</sup>U levels in global fallout. *Science of the Total Environment*, Vol. 407, pp 4238-4242
- Sanchez, A.M.; Tome, F.V.; Bejarano, J.D.; Vargas, M.J. (1992). A rapid method for determination of the isotopic composition of uranium samples by alpha spectrometry. *Nuclear Instruments and Methods in Physics Research A*, Vol. 313, pp 219-226
- Steier, P.; Golser, R.; Kutschera, W.; Liechtenstein, V.; Priller, A.; Valenta, A.; Vockenhuber, C. (2002). Heavy ion AMS with a "small" accelerator. *Nuclear Instruments and Methods in Physics Research B*, Vol. 188, pp 283-287
- Steier, P.; Bichler, M.; Fifield, L.K.; Golser, R.; Kutschera, W.; Priller, A.; Quinto, F.; Richter, S.; Srncik, M.; Terrasi, F.; Wacker, L.; Wallner, A.; Wallner, G.; Wilcken, K.M.; Wild,

- E.M. (2008). Natural and anthropogenic  $^{236}\text{U}$  in environmental samples. *Nuclear Instruments and Methods in Physics Research B*, Vol. 266, pp 2246-2250
- Steier, P.; Dellinger, F.; Forstner, O.; Golser, R.; Knie, K.; Kutschera, W.; Priller, A.; Quinto, F.; Srncik, M.; Terrasi, F.; Vockenhuber, C.; Wallner, A.; Wallner, G.; Wild, E.M. (2010). Analysis and application of heavy isotopes in the environment. *Nuclear Instruments and Methods in Physics Research B*, Vol. 268, pp 1045-1049
- Terrasi, F.; Rogalla, D.; De Cesare, N.; DŠOnofrio, A.; Lubritto, C.; Marzaioli, F.; Passariello, I.; Rubino, M.; Sabbarese, C.; Casa, G.; Palmieri, A.; Gialanella L.; Imbriani, G.; Roca, V.; Romano, M.; Sundquist, M.; Loger, R. (2007). A new AMS facility in Caserta /Italy. *Nuclear Instruments and Methods in Physics Research B*, Vol. 259, pp 14-17
- Vockenhuber, C.; Golser, R.; Kutschera, W.; Priller, A.; Steier, P.; Winkler, S.; Liechtenstein, V. (2002) Accelerator mass spectrometry of heaviest long-lived radionuclides with a 3-MV tandem accelerator, *Pramana-Journal of Physics*, Vol. 59, pp 1041-1051
- Wacker, L.; Chamizo, E.; Fifield, L.K.; Stocker, M.; Suter, M.; Synal, H.A. (2005). Measurement of actinides on a compact AMS system working at 300 kV. *Nuclear Instruments and Methods in Physics Research B*, Vol. 240, pp 452-457
- Wallner, C.; Faestermann, T.; Gerstmann, U.; Hillebrandt, W.; Knie, K.; Korschinek, G.; Lierse, C.; Pomar, C.; Rugel, G. (2000). Development of a very sensitive AMS method for the detection of supernovaproduced longliving actinide nuclei in terrestrial archives. *Nuclear Instruments and Methods in Physics Research B*, Vol. 172, pp 333-337
- Wilcken, K.M. (2006). Accelerator Mass Spectrometry of natural  $^{236}\text{U}$  and  $^{239}\text{Pu}$  with emphasis on nucleogenic isotope production. *Phd Thesis*, Australian National University, Department of Nuclear Physics, Canberra (Australia)
- Wilcken, K.M.; Barrows, T.T.; Fifield, L.K.; Tims, S.G.; Steier, P. (2007). AMS of natural  $^{236}\text{U}$  and  $^{239}\text{Pu}$  produced in uranium ores. *Nuclear Instruments and Methods in Physics Research B*, Vol. 259, pp 727-732
- Wilcken, K.M.; Fifield, L.K.; Barrows, T.T.; Tims, S.G.; Gladkis L.G. (2008). Nucleogenic  $^{36}\text{Cl}$ ,  $^{236}\text{U}$  and  $^{239}\text{Pu}$  in uranium ores. *Nuclear Instruments and Methods in Physics Research B*, Vol. 266, pp 3614-3624
- Winkler, S.R. (2008). Accelerator Mass Spectrometry of heavy radionuclides with special focus on  $^{182}\text{Hf}$ . *Phd Thesis*, Australian National University, Department of Nuclear Physics, Canberra (Australia)
- Wyse, E.J.; Lee, S.H.; Rosa, J.L.; Povinec, P.; Mora, S.J.D. (2001). ICPsector field mass spectrometry analysis of plutonium isotopes: recognizing and resolving potential interferences. *Journal of Analytical Atomic spectrometry*, Vol. 16, pp 1107-1111
- Zhao, X.L.; Nadeau, M.J.; Kilius, L.R.; Litherland, A.E. (1994). The first detection of naturally-occurring  $^{236}\text{U}$  with accelerator mass spectrometry. *Nuclear Instruments and Methods in Physics Research B*, Vol. 92, pp 249-253
- Zhao, X.-L., Kilius, L.R.; Litherland, A.E.; Beasley, T. (1997). AMS measurement of environmental U-236. Preliminary results and perspectives. *Nuclear Instruments and Methods in Physics Research B*, Vol. 126, pp 297-300



## **Nuclear Power - Control, Reliability and Human Factors**

Edited by Dr. Pavel Tsvetkov

ISBN 978-953-307-599-0

Hard cover, 428 pages

**Publisher** InTech

**Published online** 26, September, 2011

**Published in print edition** September, 2011

Advances in reactor designs, materials and human-machine interfaces guarantee safety and reliability of emerging reactor technologies, eliminating possibilities for high-consequence human errors as those which have occurred in the past. New instrumentation and control technologies based in digital systems, novel sensors and measurement approaches facilitate safety, reliability and economic competitiveness of nuclear power options. Autonomous operation scenarios are becoming increasingly popular to consider for small modular systems. This book belongs to a series of books on nuclear power published by InTech. It consists of four major sections and contains twenty-one chapters on topics from key subject areas pertinent to instrumentation and control, operation reliability, system aging and human-machine interfaces. The book targets a broad potential readership group - students, researchers and specialists in the field - who are interested in learning about nuclear power.

### **How to reference**

In order to correctly reference this scholarly work, feel free to copy and paste the following:

Mario De Cesare (2011). Origin and Detection of Actinides: Where Do We Stand with the Accelerator Mass Spectrometry Technique?, Nuclear Power - Control, Reliability and Human Factors, Dr. Pavel Tsvetkov (Ed.), ISBN: 978-953-307-599-0, InTech, Available from: <http://www.intechopen.com/books/nuclear-power-control-reliability-and-human-factors/origin-and-detection-of-actinides-where-do-we-stand-with-the-accelerator-mass-spectrometry-technique>

**INTECH**  
open science | open minds

### **InTech Europe**

University Campus STeP Ri  
Slavka Krautzeka 83/A  
51000 Rijeka, Croatia  
Phone: +385 (51) 770 447  
Fax: +385 (51) 686 166  
[www.intechopen.com](http://www.intechopen.com)

### **InTech China**

Unit 405, Office Block, Hotel Equatorial Shanghai  
No.65, Yan An Road (West), Shanghai, 200040, China  
中国上海市延安西路65号上海国际贵都大饭店办公楼405单元  
Phone: +86-21-62489820  
Fax: +86-21-62489821

© 2011 The Author(s). Licensee IntechOpen. This chapter is distributed under the terms of the [Creative Commons Attribution-NonCommercial-ShareAlike-3.0 License](https://creativecommons.org/licenses/by-nc-sa/3.0/), which permits use, distribution and reproduction for non-commercial purposes, provided the original is properly cited and derivative works building on this content are distributed under the same license.

IntechOpen

IntechOpen